

## Synthesis of long TiO<sub>2</sub> nanotube arrays with a small diameter for efficient dye-sensitized solar cells†

Cite this: *RSC Advances*, 2013, 3, 4885

Received 2nd November 2012,

Accepted 14th February 2013

DOI: 10.1039/c3ra40221e

[www.rsc.org/advances](http://www.rsc.org/advances)

Xiaolin Liu, Jia Lin and Xianfeng Chen\*

The surface/volume ratio of TiO<sub>2</sub> nanotube arrays determines their electrical, optical and chemical properties for various applications. For dye-sensitized solar cells (DSSCs), it is very important to fabricate long TiO<sub>2</sub> nanotube arrays with a larger surface area in order to have more dye loading and achieve higher conversion efficiencies accordingly. In this paper, a convenient anodization method is introduced to synthesize high aspect ratio TiO<sub>2</sub> nanotubes at a low voltage and a high temperature. With a high reaction temperature, the diffusion rate of ions in the anodization process was enhanced. At the optimum temperature, nanotubes longer than 16 μm with outside diameters as small as 75 nm could be obtained at a voltage of 20 V. Significantly, using these resulting TiO<sub>2</sub> nanotube arrays to fabricate front-side illuminated DSSCs, a conversion efficiency as high as 5.98% could be achieved due to the large surface area and the enhanced attachment of the dye.

### Introduction

One-dimensional (1D) nanostructures have been widely researched because of their high electron mobility and large specific surface area.<sup>1</sup> Compared with other metal oxides, TiO<sub>2</sub> nanotubes have attracted considerable attention owing to their excellent chemical stability, low cost and environmentally friendly features for applications such as sensing,<sup>2</sup> highly efficient photocatalysis<sup>3</sup> and dye-sensitized solar cells (DSSCs).<sup>4</sup> In developing their promising prospects for use in applications, the growth of TiO<sub>2</sub> nanotubes is an important aspect of research. Among the various preparation methods, electrochemical anodization of Ti metal is a relatively simple approach, which can easily tailor the tube length, pore diameter and wall thickness.<sup>5,6</sup>

Many attempts have been carried out to increase the surface area of TiO<sub>2</sub> nanotubes. Through infiltration with TiCl<sub>4</sub> solution

and hydrothermal synthesis, Pan *et al.* achieved uniform coating of TiO<sub>2</sub> nanoparticles 10 nm in size on the side walls of nanotubes to enlarge the surface area.<sup>7</sup> Albu *et al.* reported that double-walled TiO<sub>2</sub> nanotubes with tube wall separation could be successfully grown using a rapid thermal annealing process.<sup>8</sup> Furthermore, diminishing the pore diameter could also be an important method to improve the aspect ratio and enlarge the surface area, and some valuable efforts have been made towards the fabrication of TiO<sub>2</sub> nanotubes with small diameters. Shankar *et al.* tried to grow TiO<sub>2</sub> nanotubes in fluoride-bearing electrolytes containing different cations to get nanotubes with an aspect ratio of 700.<sup>9</sup> Using a NaF containing electrolyte, Crawford *et al.* obtained TiO<sub>2</sub> nanotubes with a length of just 650 nm and an inner diameter of about 60 nm.<sup>10</sup> Liu *et al.* fabricated 1 μm-long nanotube arrays with an open diameter of 15 nm, which improved the DSSC efficiency by 1.5%.<sup>11</sup>

However, the tubes mentioned above are not long enough for high-efficiency DSSCs. The fabrication of tubes with both adequate length and small diameter is still a great challenge. In this work, we succeeded in synthesizing TiO<sub>2</sub> nanotubes of a high aspect ratio at an elevated temperature of 50 °C and a voltage of 20 V. After anodization for a short time, TiO<sub>2</sub> nanotubes with respective inner and outer diameters of about 65 and 75 nm were successfully obtained and the thickness of the nanotube film could be increased to 16 μm. The tube diameter remained small and even slightly reduced at a high temperature. When applying these nanotubes to DSSCs, more dye is adsorbed because of the larger surface area and power conversion efficiencies as large as 5.89% were achieved consequently.

### Experimental section

Highly ordered TiO<sub>2</sub> nanotubes were fabricated through potentiostatic anodization in a conventional two-electrode electrochemical cell. The working electrode in the electrolyte was Ti foil (0.125 mm thickness, Strem Chemicals, Newburyport, MA, USA) while the counter electrode was Pt foil with a distance between the electrodes of 2 cm. Anodization was carried out under a voltage of 20 V in an electrolyte with the nominal compositions of

Department of Physics, The State Key Laboratory on Fiber Optic Local Area Communication Networks and Advanced Optical Communication Systems, Shanghai Jiao Tong University, 800 Dongchuan Road, Shanghai 200240, China.  
E-mail: [xfchen@sjtu.edu.cn](mailto:xfchen@sjtu.edu.cn)

† Electronic supplementary information (ESI) available. See DOI: 10.1039/c3ra40221e

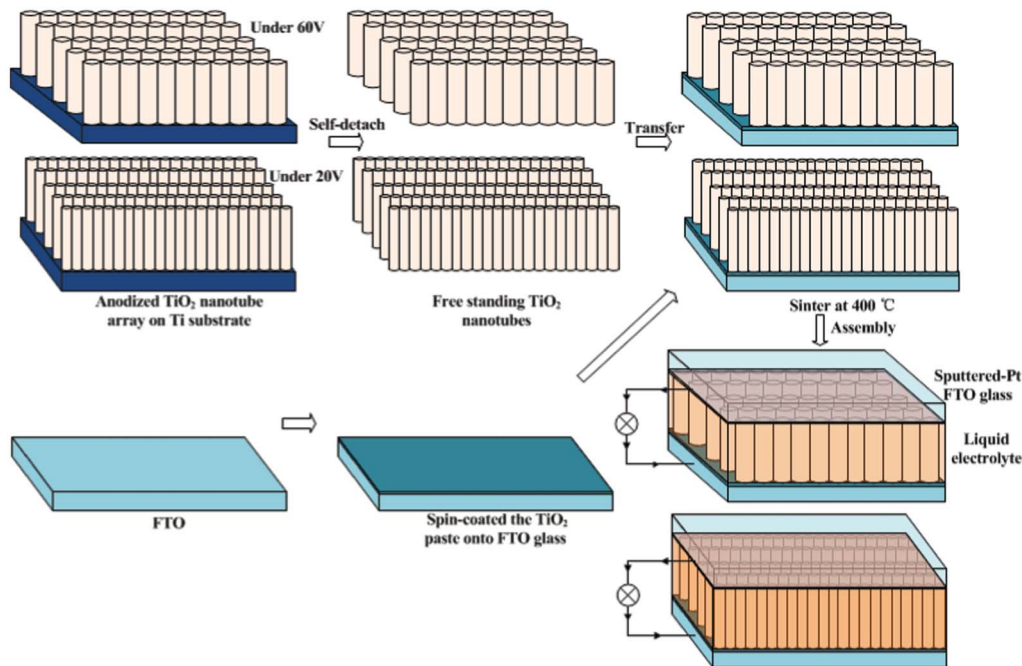


Fig. 1 Schematic of the front-side illuminated DSSC fabrication.

ethylene glycol +0.5 wt% ammonium fluoride ( $\text{NH}_4\text{F}$ ) +3 vol% deionized water. The electrolytes were kept in a water bath at constant temperatures of 20, 40, 50 and 60 °C for a duration of 1–6 h. During the reaction process, the electrolyte was stirred using a magnetic pellet throughout the duration of the reaction. For comparison, we also prepared  $\text{TiO}_2$  nanotubes at 60 V and 20 °C.

The synthesized small diameter nanotubes in our experiment were utilized to fabricate front-side illuminated DSSCs based on the free-standing membranes. A detailed fabrication process of free-standing  $\text{TiO}_2$  nanotubes has been mentioned elsewhere,<sup>12</sup> and Fig. 1 shows the schematic fabrication procedure of front-side illuminated DSSCs. The resulting oxide films were annealed at 400 °C for 1 h. Then after being anodized at a temperature of 30 °C for 0.5–1 h, free-standing membranes of high quality would form. At the same time, the  $\text{TiO}_2$  nanoparticles (P25, Degussa, Borger, TX, USA) were mixed with 3 vol% acetic acid solution in the weight ratio 3 : 10. After being stirred for 1 h, the  $\text{TiO}_2$  paste was spin-coated onto a FTO glass substrate. Then the free-standing membranes were transferred onto the substrate using tweezers immediately and sintered at 400 °C for 1 h. Then the as-formed photoanodes were immersed in a 1 : 1 (v/v) acetonitrile and *tert*-butylalcohol solution containing  $3 \times 10^{-4}$  M  $\text{RuL}_2(\text{NCS})_2\cdot 2\text{TBA}$  (N719 dye, L = 2,2'-bipyridyl-4,4'-dicarboxylic acid, TBA = tetrabutylammonium, Dyesol, Queanbeyan, New South Wales, Australia) for 48 h. A 25  $\mu\text{m}$  thick hot-melt spacer separated the sensitized electrodes and the counter electrodes which were prepared by the thermal decomposition of a  $\text{H}_2\text{PtCl}_6$  isopropanol solution on FTO glass at 420 °C for 30 min. The interspace was filled with the liquid electrolyte DMPII/LiI/I<sub>2</sub>/TBP/GuSCN in 3-methoxypropionitrile.

The structure and morphology of the  $\text{TiO}_2$  nanotubes were analyzed using field-emission scanning electron microscopy (SEM, NOVA NanoSEM 230, FEI). The active area of the solar cells in our experiment was 0.25  $\text{cm}^2$ . The amount of dye was measured through desorbing the attached dye molecules from the nanotube surface in 0.1 M NaOH aqueous solution. The absorbance was measured by a UV-vis spectrophotometer (Model UV-2550, Shimadzu, Japan) and estimated from a calibration curve of dye solutions with known concentrations. The current density–voltage ( $J$ – $V$ ) characteristics were characterized using a sourcemeter (Model 2420, Keithley, USA) under AM 1.5 G illumination (100  $\text{mW cm}^{-2}$ ) provided by a 300 W solar simulator (Model 91160, Newport-Oriel Instruments, USA) and calibrated according to a silicon reference cell (NIST) equipped with a power meter.

## Results and discussion

The current density during the tube-growing process under various conditions was measured. Fig. 2 shows the current density of the tubes as a function of the anodization time (6 h) at the temperatures of 20, 40, 50 and 60 °C under a voltage of 20 V. As shown in Fig. 2, the current density curves at different temperatures have a similar tendency. At the first stage, the narrow slits essentially follow the fluoride-free case due to the initial formation of the compact oxide layer. After that, current density decreases with the anodization time in the second step, as the regular nanotube layer forms with steady formation and dissolution processes.<sup>1</sup> In Fig. 2, we can see that the final steady-state current density at 50 °C is nearly 20  $\text{mA cm}^{-2}$ , about 10 times as much as that at 20 °C. While the current density at 60 °C has

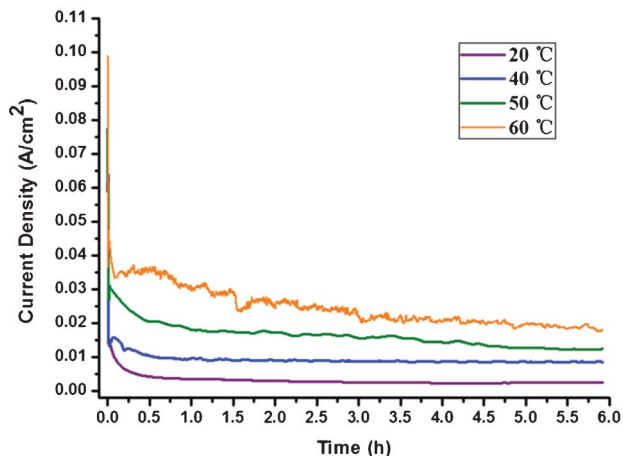


**Fig. 2** The time-dependent current density under varied anodization temperatures of 20, 40, 50 and 60 °C with a duration of 6 h.

the highest value of about 30 mA cm<sup>-2</sup>, indicating the strongest anodization reaction among the above temperatures.

The length variation of the TiO<sub>2</sub> nanotubes under different reaction conditions is presented in Fig. 3. Under 20 V and 20 °C, the tube length did not record a marked improvement with prolonged reaction time from 1 to 6 h, only increasing from 1 to 2.5 μm (Fig. 3a and c). Therefore by simply increasing the reaction time we cannot obtain long TiO<sub>2</sub> nanotubes. In contrast, an increase in tube length can be clearly seen when the bath temperature is raised, with a length of 2.8 μm after 1 h at 60 °C and 20 V (Fig. SI1a, ESI†). In our experiment, the longest tubes (up to 16.5 μm) were efficiently obtained after 6 h at 50 °C (Fig. 3d) with an approximate growth rate of about 2.7 μm h<sup>-1</sup>, which is nearly 4 times faster than the rate of 0.8 μm h<sup>-1</sup> at 20 °C. The detailed data of the length variation are listed in Table 1, demonstrating the clear effect of the reaction temperature on the tube length. It is a significant improvement that long nanotube

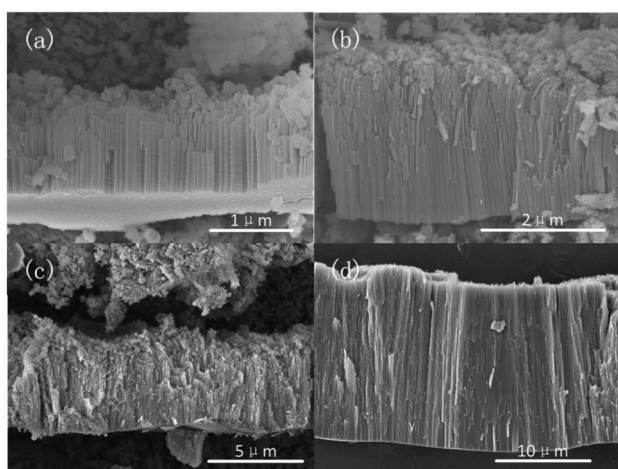


**Fig. 3** Cross-sectional SEM images of the highly ordered TiO<sub>2</sub> nanotube arrays from different reaction conditions: (a, b) 20 V, 20 °C and 50 °C for 1 h and (c, d) 20 V, 20 °C and 50 °C for 6 h.

arrays are prepared with a fast growth rate while maintaining their small diameters at the same time (as can be seen in Table 1), which was achieved simply using a high temperature and a low applied voltage. Further increasing the anodization temperature (60 °C) does not lead to longer tubes (Fig. SI1b, ESI†), which may be caused by excessive chemical dissolution at the elevated temperature.

The variation of tube diameter under different reaction temperatures can be observed in the side-view SEM results presented in Fig. 4. As reported before, the tube diameter is affected by the applied voltage with a constant linear factor ratio.<sup>13</sup> The outer and inner diameters of the tubes prepared at 20 °C and 60 V in our experiment are about 152 and 88 nm, respectively. While reducing the voltage to 20 V, the diameters decreased to be just 93 and 67 nm (Fig. 4a and d). However, as electrochemical etching at high field strength is prominent, while chemical dissolution at low field strength dominates the growth process,<sup>14</sup> the growth rate would decrease along with lowering the voltage to obtain the small tube diameter, which limits the tube length. Thus in our experiment, we use an elevated reaction temperature to accelerate the tube growth under the same low reaction voltage values. An important advantage of our method is that the tube diameter remains small and even slightly reduced at higher temperatures. As shown in Fig. 3c, after anodization at 50 °C and 20 V for 6 h, the outer and inner diameters of the resulting tubes are 75 nm and 65 nm respectively, the outer diameters of which are reduced by ~19% compared with the samples prepared at 20 °C and 20 V. The detailed information is also listed in Table 1.

From the above discussion, it can be clearly seen that besides the anodization time and the applied voltage, the reaction temperature also plays a crucial role in the variation of the tube length and diameter. At low voltage, the formation of a thick barrier layer at the bottom of the tubes inhibits further ion diffusion and tube growth.<sup>15</sup> Thus simply prolonging the reaction time from 1 to 6 h could only lead to the tubes lengthening from 1 μm to 2.5 μm. However, if the reaction is carried out at a higher temperature, the viscosity of the reaction solution would become less dense and all of the metal-, oxygen- and F-ions would be transported faster, which could also be demonstrated by the higher current density shown in Fig. 2. As a fraction of the ionic current at the film-solution interface contributes to the oxide growth,<sup>16</sup> longer nanotubes can be obtained at a higher temperature given a specific period of reaction time. At the same time, stirring the electrolyte during the reaction would help to increasing the tube length because of better ionic transportation caused by more metal cations being incorporated in the oxide.<sup>17</sup> Furthermore, the increased amount of F<sup>-</sup> at the bottom accelerates the dissolution of the barrier layer, leading to the thinner tube walls and a smaller tube outer diameter,<sup>18</sup> as the tube outer diameter changed from 93 to 75 nm when the temperature was increased from 20 to 50 °C.

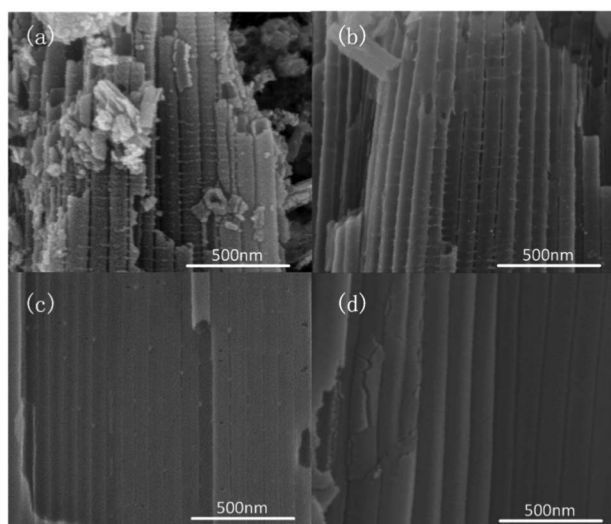
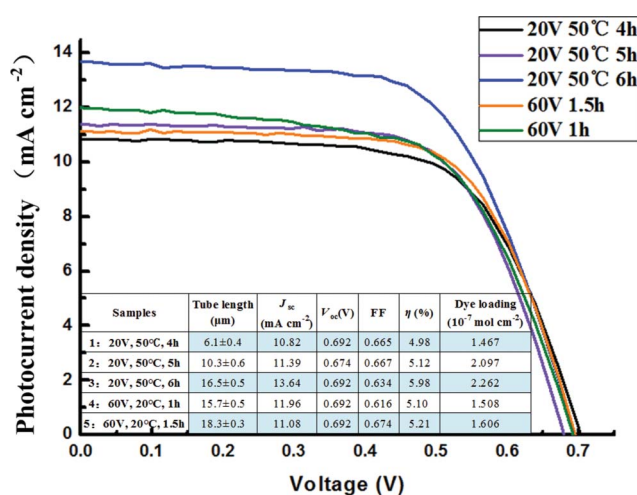
The nanotubes with different diameters and lengths were incorporated into DSSCs. A total of 2–4 cells were tested for each type of cell. Their typical photocurrent density-voltage (*J*-*V*) curves are plotted in Fig. 5, with a table of detailed results inserted. Fig. SI2, ESI† shows the cross-sectional SEM images of the DSSCs'

**Table 1** Diameter and length of the nanotubes resulting from different reaction conditions

Anodization voltage (V)	T (°C)	Duration	Tube outer diameter (nm)	Tube inner diameter (nm)	Tube length (μm)
20	20	6 h	93 ± 5	67 ± 6	4.75 ± 0.50
20	40	6 h	81 ± 5	69 ± 1	7.55 ± 0.80
20	50	6 h	75 ± 2	65 ± 2	16.50 ± 0.50
60	20	1 h	152 ± 11	88 ± 3	15.70 ± 0.50

photoanodes which have approximately the same TiO<sub>2</sub> nanoparticle layer thickness of ~2 μm, in order to avoid the influence of the thickness of the TiO<sub>2</sub> paste. Similar open-circuit voltage ( $V_{oc}$ ) and fill factor (FF) values were exhibited by the small tubes (Sample 3) and large tubes (Sample 4) of similar length, while the short-circuit current density ( $J_{sc}$ ) increased by 25% (from 11.96 to

13.64 mA cm<sup>-2</sup>). Owing to the large improvement of  $J_{sc}$ , the small tubes yield a considerably higher conversion efficiency ( $\eta$ ), which is improved from 5.1 to 5.98% (increased by nearly 17%). Moreover the large tubes (Sample 5) with the longest tube length in our experiment still had a lower efficiency than Sample 3 (smaller by 15%). It is also noticeable that the amount of dye attached in Sample 3 could be enhanced by 50% over that in Sample 4. Meanwhile the dark current data in Fig. S13, ESI† indicate that the DSSCs with tubes of smaller diameters have a higher dark current. As tubes with small diameters always have a large surface area which can lead to more dye loading than large diameter tubes with similar or longer tube lengths, the enhancement of light harvesting and significant improvement in  $J_{sc}$  and efficiency are expected. The debris-free surfaces of the long tubes (Fig. 3d) may also contribute to the improved efficiency. Therefore the fabrication of DSSCs with better performance presented in our work is simple and efficient.

**Fig. 4** Side views of the highly ordered nanotubes: (a) 20 °C, (b) 40 °C, (c) 50 °C, for 6 h at 20 V and (d) 20 °C, for 1 h at 60 V.**Fig. 5**  $J$ - $V$  curves of DSSCs based on five different kinds of TiO<sub>2</sub> nanotubes processed at 20 V and 60 V with different diameters and lengths (inset: the values of  $J_{sc}$ ,  $V_{oc}$ , FF,  $\eta$ , and dye loading of the DSSC samples).

## Conclusion

In this work, a simple preparation method for TiO<sub>2</sub> nanotubes with a high aspect ratio has been achieved successfully. TiO<sub>2</sub> nanotubes with good properties can be easily fabricated by increasing the anodization temperature. The elevated reaction temperature can lower the viscosity of the electrolyte, enhance the chemical dissolution and accelerate the electrochemical formation. After anodization at an elevated temperature of 50 °C and a voltage of 20 V for 6 h, the resulting tubes with an outer diameter of 75 nm are more than 16 μm long, much longer than the 2.5 μm-long tubes processed at the original temperature of 20 °C. Long nanotubes with small diameters can lead to more dye attachment and efficiently improve the capability of DSSCs. Using the fabricated nanotubes in DSSCs results in the conversion efficiency of the DSSCs being remarkably increased to as high as 5.98%.

## Acknowledgements

The work was supported by the National Natural Science Foundation of China (Grant No. 61125503) and the Foundation for Development of Science and Technology of Shanghai (Grant No. 11XD1402600, No. 10JC1407200).

## References

- 1 P. Roy, S. Berger and P. Schmuki, *Angew. Chem., Int. Ed.*, 2011, **50**, 2904.
- 2 O. K. Varghese and C. A. Grimes, *J. Nanosci. Nanotechnol.*, 2003, **3**, 277.

- 3 S. Livraghi, A. Votta, M. C. Paganini and E. Giamello, *Chem. Commun.*, 2005, 498.
- 4 J. M. Macak, H. Tsuchiya, A. Ghicov and P. Schmuki, *Electrochem. Commun.*, 2005, 7, 1133.
- 5 G. K. Mor, K. Shankar, M. Paulose, O. K. Varghese and C. A. Grimes, *Nano Lett.*, 2005, 5, 191.
- 6 L. Sun, S. Zhang, X. Sun and X. He, *J. Nanosci. Nanotechnol.*, 2010, 10, 4551.
- 7 X. Pan, C. Chen, K. Zhu and Z. Fan, *Nanotechnology*, 2011, 22, 235402.
- 8 S. P. Albu, A. Ghicov, S. Aldabergenova, P. Drechsel, D. LeClere, G. E. Thompson, J. M. Macak and P. Schmuki, *Advanced Materials*, 2008, 20, 4135.
- 9 K. Shankar, G. K. Mor, A. Fitzgerald and C. A. Grimes, *J. Phys. Chem. C*, 2007, 111, 21.
- 10 G. Crawford, N. Chawla, K. Das, S. Bose and A. Bandyopadhyay, *Acta Biomater.*, 2007, 3, 359.
- 11 N. Liu, K. Lee and P. Schmuki, *Electrochem. Commun.*, 2012, 15, 1.
- 12 J. Lin, J. Chen and X. Chen, *Electrochem. Commun.*, 2010, 12, 1062.
- 13 S. Bauer, S. Kleber and P. Schmuki, *Electrochem. Commun.*, 2006, 8, 1321.
- 14 L. Sun, S. Zhang, X. W. Sun and X. He, *J. Electroanal. Chem.*, 2009, 637, 6.
- 15 J. Ou, R. A. Rani, M. Ham, M. R. Field, Y. Zhang, H. Zheng, P. Reece, S. Zhuiykov, S. Sriram, M. Bhaskaran, R. B. Kaner and K. Kalantar-zadeh, *ACS Nano*, 2012, 6, 4045.
- 16 K. R. Hebert, S. P. Albu, I. Paramasivam and P. Schmuki, *Nat. Mater.*, 2011, 11, 162.
- 17 R. Narayanan, T. Y. Kwon and K. H. Kim, *Mater. Lett.*, 2009, 63, 2003.
- 18 Q. Van Overmeere, F. Blaffart and J. Proost, *Electrochem. Commun.*, 2010, 12, 1174.